Int J Environ Res (2022) 16:8
https://doi.org/10.1007/s41742-021-00388-0

RESEARCH PAPER

Removal of Phosphate from the Healthcare Wastewater Through Peroxi-Photoelectrocoagulation Process: Effect of Process Parameters

Samuel Fekadu[1,2,4] · **Esayas Alemayehu**[2,5] · **Perumal Asaithambi**[2] · **Bart Van der Bruggen**[1,3]

Received: 26 August 2021 / Revised: 11 December 2021 / Accepted: 25 December 2021

Abstract

Among various anionic pollutants encountered in many wastewater effluents, phosphate is an important one. Excessive concentration levels of phosphate must be reduced from wastewater to prevent effects on aquatic ecosystems. In the present work, a peroxi-photoelectrocoagulation process was employed to determine the phosphate removal efficiency. Bench-scale experiments were performed in an electrolytic cell. A total of thirty-seven experiments were conducted using full factorial design with center points to examine the effect of the process parameters, i.e., initial phosphate, pH, reaction time, hydrogen peroxide and current density for response variables of phosphate removal efficiencies and energy consumption. The result obtained from the experiment runs shows that the percentage removal of phosphate ranges between 38.46–97.91% and the concentration of phosphate dropped up to the level of 0.12 mg L^{-1}. The electric energy consumed in the treatment processes ranges between 0.27–5.94 kWh/g-P. The energy consumption per load of removed phosphate was found to depend on the initial phosphate concentration, pH, RT and current density.

Graphical abstract

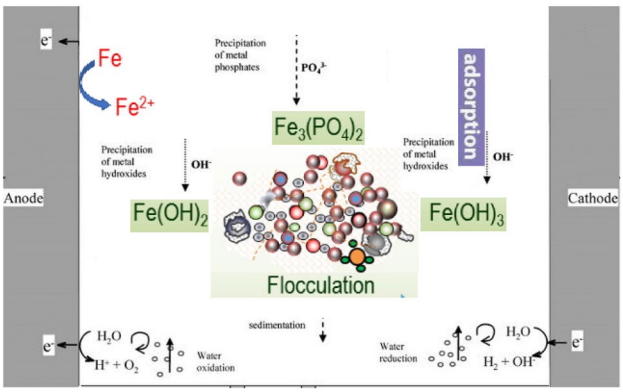

Article highlights

- The percentage removal of phosphate reached up to 98%.
- The process brings down the phosphate concentration level up to 0.12 mg L^{-1}.
- In peroxi-photoelectrocoagulation process, phosphate removal was increased with pH.
- The electric energy consumed in the process ranges 0.27–5.94 kWh/g-P.

Keywords Electrochemical oxidation · Healthcare wastewater · UV · Hydrogen peroxide · Phosphate removal · Factorial design

✉ Samuel Fekadu
samuel.fekadu@ju.edu.et

Extended author information available on the last page of the article

Published online: 05 January 2022

Introduction

The composition of wastewater varies among different sources and over time. The concentration ranges measured in healthcare effluents collected in different geographic regions over 20 years shows the higher impact of this effluent as a source of inorganic/organic matter loads, particularly when compared with municipal effluent (Verlicchi et al. 2018). The healthcare effluents typically present physicochemical parameters such as BOD_5, COD, and TSS two to three times higher than municipal effluents (Verlicchi et al. 2010). Among various anionic pollutants which could be generally encountered in many wastewater effluents, phosphate is an important one. Most of the recent nutrient-removal studies have focused on the removal of phosphate, as it's the limiting factor in the eutrophication process (Cui et al. 2021).

Phosphate present in the healthcare wastewater (HCWW) measured up to 19 mg P-PO_4 L^{-1} (Verlicchi et al. 2018). Phosphate (PO_4^{3-}) is an essential nutrient that stimulates the growth of photosynthetic organisms like planktonic cyanobacteria and algae (Lin et al. 2021), however, excessive concentration levels must be reduced from wastewater to prevents effects on aquatic ecosystems and severe threats to drinking water supplies (Mahmud et al. 2020; Lin et al. 2021). Its abundance can accelerate eutrophication in many aquatic environments (Jung et al. 2015; Lee et al. 2017). These severe environmental concerns linked to phosphate pollution have become an essential subject for its removal from wastewater streams (Mohan et al. 2014; Mahdavi and Akhzari 2016; Chen et al. 2018). EPA recommends a maximum 0.025 mg L^{-1} phosphate concentration for lakes or reservoirs (USEPA 1986) if exceed this value promote excessive or harmful algal blooms and other aquatic plants.

Commonly, there are two categories of approach to phosphate removal from wastewaters (physicochemical and biological) (Zhang et al. 2018; Bouamra et al. 2018; Šikić et al. 2019; Mazloomi et al. 2019; Besharati Fard et al. 2020). As of the good performance and low cost, there is a widespread application of the biological processes (Yang et al. 2017), even though, high removal rate greatly depends on precise control of operational parameters (Zuthi et al. 2013). Coagulation and flocculation are a typical physicochemical process that is mostly applied for phosphate removal (Zhang et al. 2018). Different electrochemical methods (e.g., electrocoagulation) have been found effective for the removal of various anionic pollutants (such as phosphate, cyanide, fluoride, nitrate, nitrite and sulfate) from water and wastewater (Lacasa et al. 2011; Pulkka et al. 2014; Ouslimane et al. 2017). In the past few years, removal of phosphate via electrocoagulation processes have been investigated by several studies (Attour et al. 2016; Đuričić, et al. 2016; Tian et al. 2017; Al-Raad and Hanafiah 2021) and has been flagged as promising cost-effective in its high phosphate removal efficiency. In the present work, a peroxi-photoelectrocoagulation process was employed to determine the phosphate removal efficiency. In this process, electrocoagulation is combined with UVc light and hydrogen peroxide.

This study aims to determine the optimum operating conditions such as initial phosphate concentration, the amount of H_2O_2 added, reaction time, current density and initial pH of the wastewater for the removal of phosphate from waters by the peroxi-photoelectrocoagulation process with iron plate electrodes. A predictive model for phosphate removal was suggested. Furthermore, the energy consumption in the system was evaluated for removing phosphate.

Materials and Methods

Chemicals

Hydrogen peroxide, 30% was supplied by Finkem Laboratory Reagent (India). Glass microfibre filters (Grade 934-AH) were supplied by Whatman. Deionized water was used to dilute the wastewater in the experimental runs as needed. Sulphuric acid (98.08%) was purchased from Finkem Laboratory Reagent (India). For the stannous chloride method: phenolphthalein indicator, ammonium molybdate reagent, stannous chloride reagent, stock phosphate solution and standard phosphate solution were prepared by chemicals supplied by Fisher Scientific (UK).

Sampling

The wastewater sample was taken from the septic tank effluent of Jimma University Specialized Hospital (JUSH) in Jimma town, Ethiopia. The town is located at 7° 41' N latitude and 36° 50' E longitudes and an average altitude of about 1780 m above sea level. The collected 50 L sample was stored in a refrigerator at 4 °C until the experiment was ended. Before each experiment run, the wastewater was diluted as needed with deionized water to meet the initial phosphate concentration shown in Table 1. The

Table 1 The level of process parameters selected

Process parameters	Low level	Center point	High level
Initial phosphate (mg L^{-1})	1.43	3.58	5.73
H_2O_2 (mg L^{-1})	150	225	300
pH	3	6	9
Reaction time (min)	30	45	60
Current density (mA cm^{-2})	3.5	5.25	7

initial phosphate concentration of the raw wastewater was 5.73 mg L^{-1}.

Experimental Setup and Procedure

The experimental setup was arranged based on our previous works (Fekadu et al. 2021a, b). Bench-scale experiments were performed in an electrolytic cell equipped with two stainless-steel electrodes each having a 28 cm^2 effective surface area. For enhanced electrical performance two extra stainless-steel plates with the same dimensions were placed between the anode and the cathode (Fekadu et al. 2021a). The gap between the plates was 0.5 cm. The schematic of the batch experimental setup is presented in Fig. 1. The electrical current was applied using a DC power supply. In all experiments, UVc lamp (6 W) was used as a source of irradiation, which was placed 15 cm above the reactor. In each experiment, 1 L of HCWW was fed to the reactor. To ensure homogeneity and disperse the coagulant matter in the reactor efficiently the magnetic stirrer was used that adjusted at 250 rpm. The pH 3310 from Xylem Analytics Germany GmbH was used to monitor pH, and the wastewater pH was adjusted to the desired level using NaOH (0.1 M) and H_2SO_4 (0.1 M). The phosphate concentration in the wastewater was determined by the stannous chloride method, according to the standard methods (APHA 2017). The concentration before and after treatment was measured using DR 5000™ UV–Vis Spectrophotometer after calibration has been made with deionized water for each run. To ensure the precision of the results, the measurements were done in duplicate.

Analysis: Phosphate Removal Efficiency

The percentage of phosphate removal in the solution is determined using Eq. (1):

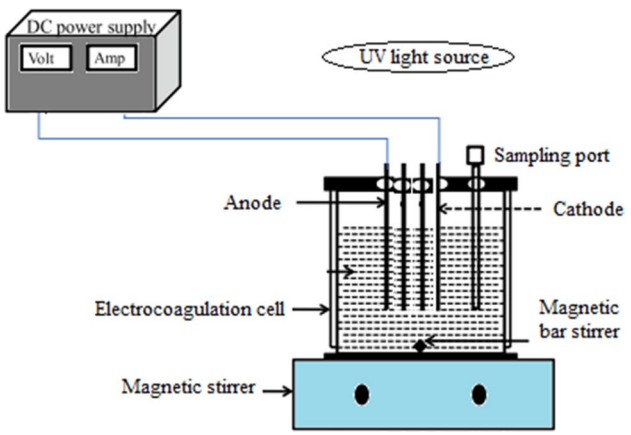

Fig. 1 Schematic representation of the experimental setup (Fekadu et al. 2021b)

$$\eta = \left[\left(P_0 - P_t\right)/P_0\right] \times 100, \quad (1)$$

where η is the phosphate removal efficiency (%), P_0 is the phosphate concentration before treatment (mg L^{-1}), P_t is the phosphate concentration after treatment (mg L^{-1}).

Analysis: Energy Consumption

The energy consumption (E) in the phosphate removal process was calculated for each experimental run by Eq. (2) (Rodziewicz et al. 2020).

$$E = UIt/\left[\left(P_0 - P_t\right) \times V\right], \quad (2)$$

where E is the energy consumption (kWh/g phosphate removed), U is the voltage applied (V), I is the current (A), t is the reaction time (h), V is the volume of treated wastewater (L).

Design of Experiments

A total of thirty-seven experiments was conducted using full factorial design with center points to examine the effect of the process parameters, i.e., initial phosphate, pH, reaction time, hydrogen peroxide and current density for response variables of phosphate removal efficiencies and energy consumption (Table 1). To create higher process stability and to check for curvature, five center points were added (SEMATECH 2003). The analysis of the experimental data was supported by the statistical package JMP pro-15.0.

Results and Discussion

Five input variables; initial phosphate concentration, pH, reaction time, hydrogen peroxide and current density were designated in the experimental design. This experimental plan was conducted with the 2-level full factorial design that resulted 37 experiments. The number of experiments (N) determined using the formula $N = 2^{k} + C_0$, where k is the number of input variables and C_0 is the number of center point runs. All the conducted experiments are shown in Table 2, the levels for each variable; − 1, 0 and 1 signs match to the low, center and high values of the variables, respectively. The response of percentage phosphate removal and energy consumption together with their predictive values also presented in this Table.

Model Development and Validation

To develop and validate the models the same procedure were followed as of our previous work (Fekadu et al. 2021b). The statistical package JMP pro 15 has been used as a statistical

Table 2 Observed response; phosphate removal and energy consumption for the 2^5factorial experimental design with 5 center points

Run	Pattern	Initial Phosphate (mg L−1)	H_2O_2 (mg L−1)	pH	RT (min)	Current density (mA cm^{-2})	Phosphate removal (%)	Predicted phosphate removal (%)	Energy consumption (kWh/g-P)	Predicted energy consumption (kWh/g-P)
1	+ + − + −	1	1	− 1	1	− 1	94.59	95.04	0.55	0.52
2	00000	0	0	0	0	0	83.24	84.24	1.13	1.85
3	+ − + − +	1	− 1	1	− 1	1	93.72	95.00	0.56	0.50
4	00000	0	0	0	0	0	91.34	84.24	1.03	1.85
5	− − + + +	− 1	− 1	1	1	1	70.63	80.70	5.94	4.53
6	− − + − −	− 1	− 1	1	− 1	− 1	90.91	91.31	1.15	0.97
7	− + + − −	− 1	1	1	− 1	− 1	90.21	91.31	1.16	0.97
8	− + − + −	− 1	1	− 1	1	− 1	67.13	73.53	3.13	3.22
9	− − − + −	− 1	− 1	− 1	1	− 1	69.23	73.53	3.03	3.22
10	+ + − − +	1	1	− 1	− 1	1	95.29	94.65	0.55	0.52
11	− + − − −	− 1	1	− 1	− 1	− 1	60.14	45.56	1.74	1.84
12	− − + + −	− 1	− 1	1	1	− 1	84.62	86.60	2.48	2.34
13	+ − − + +	1	− 1	− 1	1	1	86.21	89.15	1.21	0.96
14	+ + + + +	1	1	1	1	1	95.11	98.14	1.10	0.94
15	− − − + +	− 1	− 1	− 1	1	1	85.31	79.42	4.92	5.41
16	− + − + +	− 1	1	− 1	1	1	80.42	79.42	5.22	5.41
17	− − − − −	− 1	− 1	− 1	− 1	− 1	38.46	45.56	2.73	1.84
18	+ + + − +	1	1	1	− 1	1	94.42	95.00	0.55	0.50
19	− − + − +	− 1	− 1	1	− 1	1	79.72	85.42	2.63	3.16
20	+ + − + +	1	1	− 1	1	1	86.39	89.15	1.21	0.96
21	+ + + + −	1	1	1	1	− 1	91.8	92.24	0.57	0.50
22	00000	0	0	0	0	0	93.02	84.24	1.01	1.85
23	− + + + +	− 1	1	1	1	1	84.62	80.70	4.96	4.53
24	+ − − − +	1	− 1	− 1	− 1	1	95.46	94.65	0.55	0.52
25	+ − − + −	1	− 1	− 1	1	− 1	97.38	95.04	0.54	0.52
26	− + + + −	− 1	1	1	1	− 1	90.91	86.60	2.31	2.34
27	− − − − +	− 1	− 1	− 1	− 1	1	50.35	51.45	4.17	4.04
28	+ − − − −	1	− 1	− 1	− 1	− 1	97.91	100.54	0.27	0.08
29	+ + + − −	1	1	1	− 1	− 1	86.91	89.10	0.30	0.07
30	− + + − +	− 1	1	1	− 1	1	88.81	85.42	2.36	3.16
31	00000	0	0	0	0	0	92.46	84.24	1.02	1.85
32	+ + − − −	1	1	− 1	− 1	− 1	97.91	100.54	0.27	0.08
33	00000	0	0	0	0	0	91.62	84.24	1.03	1.85
34	+ − + + +	1	-1	1	1	1	94.76	98.14	1.11	0.94
35	− + − − +	-1	1	-1	-1	1	41.26	51.45	5.08	4.04
36	+ − + + −	1	-1	1	1	-1	95.29	92.24	0.55	0.50
37	+ − + − −	1	-1	1	-1	-1	89.35	89.10	0.29	0.07

tool to model the variation of phosphate removal and energy consumption with the change in the operating parameters. A full factorial experimental design was applied to find the statistically significant variables on the responses. To have as simple as possible models that can accurately describe the process the model terms with low significant (p value > 0.05) were removed from the models. The model term with the highest p value were removed first from the model by retain the regression coefficients value (R^2) not to be below 0.8. The regression coefficients value was reduced from 0.97 to 0.88 and 0.96 to 0.91 for phosphate removal and energy consumption, respectively, while eliminating the model term with the highest p value.

The obtained reduced models for phosphate removal and energy consumption can still define the process sufficiently, as supported by the predicted and experimental value. These two values are in a good agreement for obtained reduced models of both responses (Fig. 2A, B). Which is evidenced

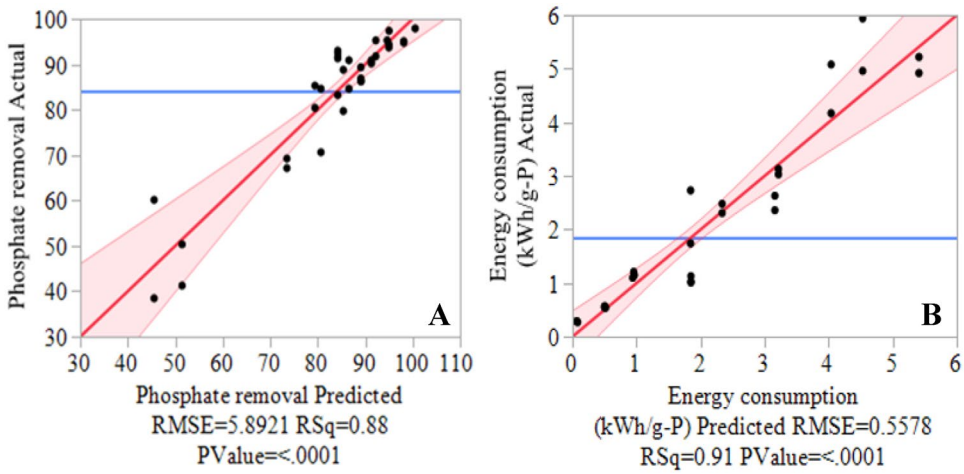

Fig. 2 Plot showing the relationship between experimental and predicted values for % phosphate removal (**A**) and energy consumption (**B**)

Table 3 Analysis of variance for phosphate removal and energy consumption

Source	DF	Sum of squares	Mean square	*F* ratio
For phosphate removal				
Model	8	7380.9914	922.624	26.5761
Error	28	972.0565	34.716	Prob > F
C. Total	36	8353.0479		< 0.0001*
For energy consumption				
Model	7	88.717697	12.6740	40.7276
Error	29	9.024460	0.3112	Prob > F
C. Total	36	97.742157		< 0.0001*

by the regression coefficients of determination greater than 0.8 that revealed the satisfactory predictions (Bucchianico 2014). The ANOVA analysis also exhibited that the two models were significant and predict well the % of phosphate removal and energy consumption (Table 3).

Tables 4 and 5 includes a threshold value for noticing the most significant terms for the phosphate removal and energy consumption as revealed in a vertical blue line, that set at the value 2, on the LogWorth horizontal bar chart. A LogWorth that surpasses 2 is significant at the 0.01 level. For the phosphate removal model (Table 4) demonstrates that; the effects are significant at the 0.01 level except for reaction time, which is significant at the 0.05. In this partially reduced model of phosphate removal shows that the initial phosphate, pH and reaction time are the three main effects that have a significant influence on phosphate reduction from the treated wastewater. This model with the eight terms also indicates that interactions have a significant influence. The first-order interaction of initial phosphate with pH and reaction time; and pH with reaction time has a significant interaction effect. The model also illustrates that the second-order interactions of initial phosphate, pH and reaction time; and initial phosphate, pH and current density has a significant influence in reducing phosphate from the treated wastewater.

Table 4 Effect summary for the partially reduced model for phosphate removal

Source	LogWorth	*p* value
Initial Phosphate	9.623	0.00000
Initial Phosphate * pH	5.665	0.00000
pH	4.973	0.00001
Initial Phosphate * pH* RT	4.509	0.00003
Initial Phosphate *RT	2.330	0.00468
pH * RT	2.129	0.00743
Initial Phosphate * pH * Current density	2.071	0.00850
RT	1.739	0.01824

Table 5 Effect summary for the partially reduced model for energy consumption

Source	LogWorth	*p* value
Initial Phosphate	13.366	0.00000
Current density	6.589	0.00000
RT	4.096	0.00008
Initial Phosphate * Current density	3.936	0.00012
Initial Phosphate * RT	1.605	0.02481
pH	1.507	0.03111
Initial Phosphate * pH	1.435	0.03674

Table 6 Suggested models for phosphate removal

Term	Estimate	Std Error	t Ratio	Prob>|t|
Intercept	84.240811	0.968648	86.97	<.0001*
Initial Phosphate	9.9928125	1.041578	9.59	<.0001*
pH	5.5734375	1.041578	5.35	<.0001*
Initial Phosphate * pH	− 6.184688	1.041578	− 5.94	<.0001*
RT	2.6115625	1.041578	2.51	0.0182*
Initial Phosphate * RT	− 3.201563	1.041578	− 3.07	0.0047*
pH * RT	− 3.005937	1.041578	− 2.89	0.0074*
Initial Phosphate * pH * RT	5.1659375	1.041578	4.96	<.0001*
Initial Phosphate * pH * Current density	2.9484375	1.041578	2.83	0.0085*

Table 7 Suggested models for energy consumption

Term	Estimate	Std Error	t Ratio	Prob>|t|
Intercept	1.8489189	0.091709	20.16	<.0001*
Initial Phosphate	− 1.338438	0.098614	− 13.57	<.0001*
pH	− 0.223438	0.098614	− 2.27	0.0311*
Initial Phosphate * pH	0.2159375	0.098614	2.19	0.0367*
RT	0.4521875	0.098614	4.59	<.0001*
Initial Phosphate * RT	− 0.233438	0.098614	− 2.37	0.0248*
Current density	0.6578125	0.098614	6.67	<.0001*
Initial Phosphate * Current density	− 0.439063	0.098614	− 4.45	0.0001*

In the model of energy consumption (Table 5), seven terms have a significant effect that were judged by *p*-values (less than 0.05). As can be seen from Table 5, the first four terms were very highly significant since the *p*-values were < 0.01 (namely: initial phosphate, current density, reaction time and the interaction effect of initial phosphate with current density). The energy consumption for the removal of phosphate from the wastewater also predisposed by another main effect (i.e., pH) and by first-order interaction (initial phosphate with RT and pH) at a significant level of 0.05. The estimates of the suggested models that describe phosphate removal and energy consumption are presented in Tables 6 and 7.

Operational Parameters Affecting Phosphate Removal

The peroxi-photoelectrocoagulation process efficiency as a function of various input variables with their low and high levels give in a range of result on phosphate removal and energy consumption (Table 2). The result of 37 experiment runs showed that the percentage removal of phosphate range 38.46 to 97.91% and the concentration of phosphate dropped up to the level of 0.12 mg L^{-1}. The operating parameters studied are discussed in this section.

Influence of the Initial Phosphate Concentration

Sets of wastewater samples with three different concentrations of phosphate (1.43, 3.58 and 5.73 mg L^{-1}) were treated. As can be seen in the prediction profiler (Fig. 3) the removal efficiency is directly proportional to the initial concentration of phosphate, where the removal efficiency increases with the initial concentration of phosphate. This could be because of the availability of enough flocs to absorb all the phosphate ions within the experimental concentration ranges. This may not be the case while using the higher concentration range of initial phosphate (For instance; up to 150 mg L^{-1} using a synthetic phosphate solution) as reported in research work of Hashim et al. (2019).

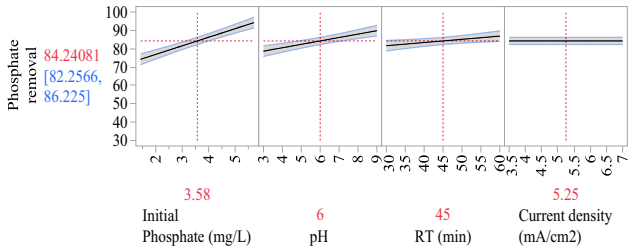

Fig. 3 Prediction profiler of phosphate removal (The vertical red lines correspond to the current value of the factors. The current value of each factor is also shown in red below the horizontal axis. The red value on the vertical axis is the predicted response based on the current values of the factors)

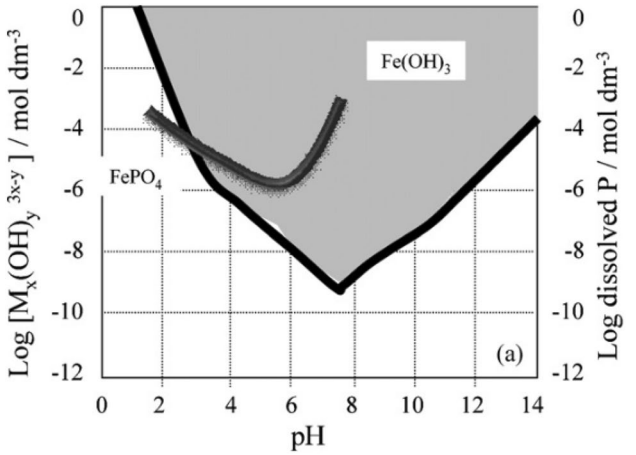

Fig. 5 Solubility diagram of iron phosphate and iron hydroxide as a function of pH

Influence of the pH

The influence of pH on phosphate removal has been investigated by treating phosphate-containing wastewater of different initial pH values (3, 6 and 9). The pH was adjusted using either sodium hydroxide or sulfuric acid as needed. Figure 4 illustrates that as a pH increase from 3 to 9, the phosphate removal also increased. This is due to an incremental of the adsorption of phosphate onto the iron hydroxide as pH increases. As can be seen on the diagram (Fig. 5) that have been widely reported in the literature (Lacasa et al. 2011), shows the solubility of iron and phosphate insoluble precipitates as a function of pH. This diagram depicts that, as pH increase, phosphate was noticed to be removed by iron hydroxides precipitation rather than forming iron phosphate. Iron phosphates have a higher solubility than iron hydroxides and adsorption of phosphate onto the iron hydroxide is a significant pathway in the phosphate removal (Pulkka et al. 2014). Thus, in peroxi-photoelectrocoagulation process for removing phosphates completely was increased with pH.

Influence of the Reaction Time and Current Density

In the present study, the elimination of phosphate slightly increased with time (Fig. 3). The interaction effect of RT with initial phosphate concentration is shown in Fig. 6. As can be seen in this figure, at lower initial phosphate concentration (i.e., <3 mg L^{-1}), required 60 min of treatment time to remove up to 85% of phosphate. While at the higher initial concentration (i.e., >3 mg L^{-1}) 30 min is enough to remove up to 95% of phosphate. This might be due to the formation of larger floc at a higher initial concentration within a shorter treatment time. The initial pH of the wastewater is another factor that shows interaction with RT (Fig. 7). At a higher initial pH, 30 min of treatment time is enough for the

Fig. 4 Response surface plot and two-dimension contour for interaction between initial phosphate concentration and pH with other value fixed to center points

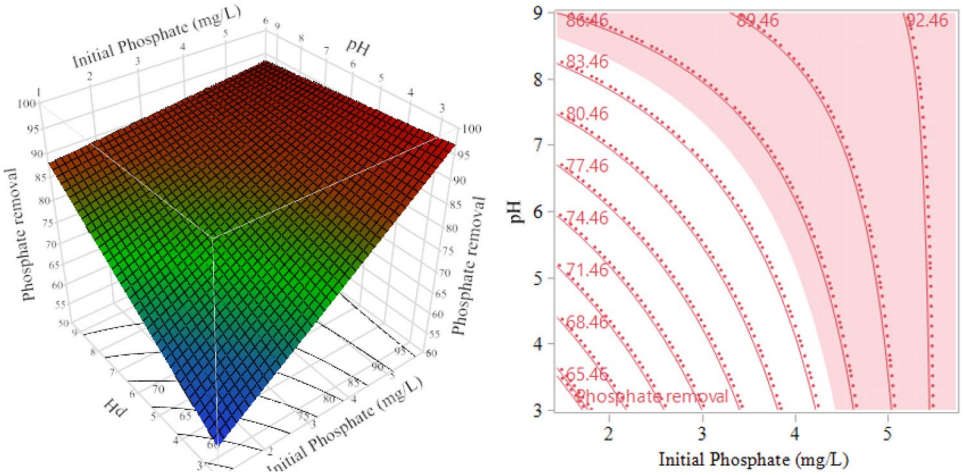

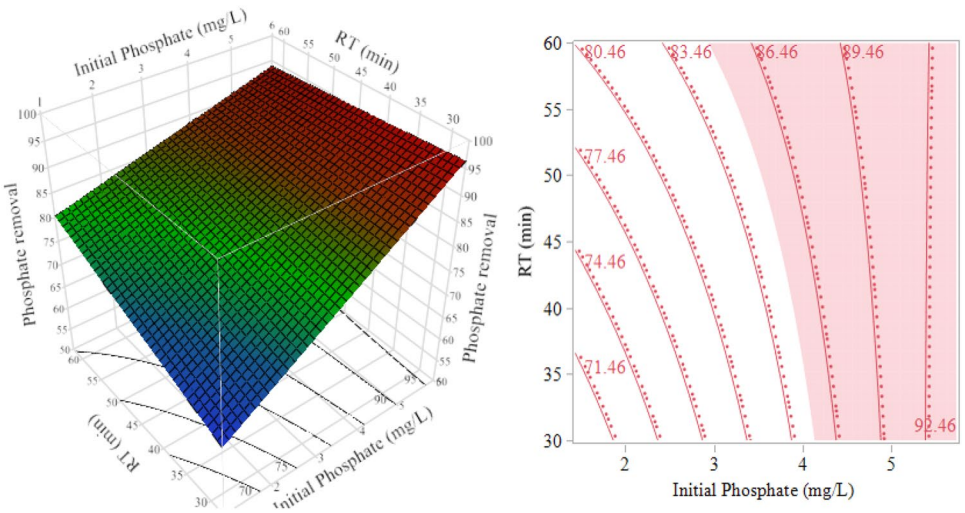

Fig. 6 Response surface plot and two-dimension contour for interaction between initial phosphate concentration and RT with other value fixed to center points

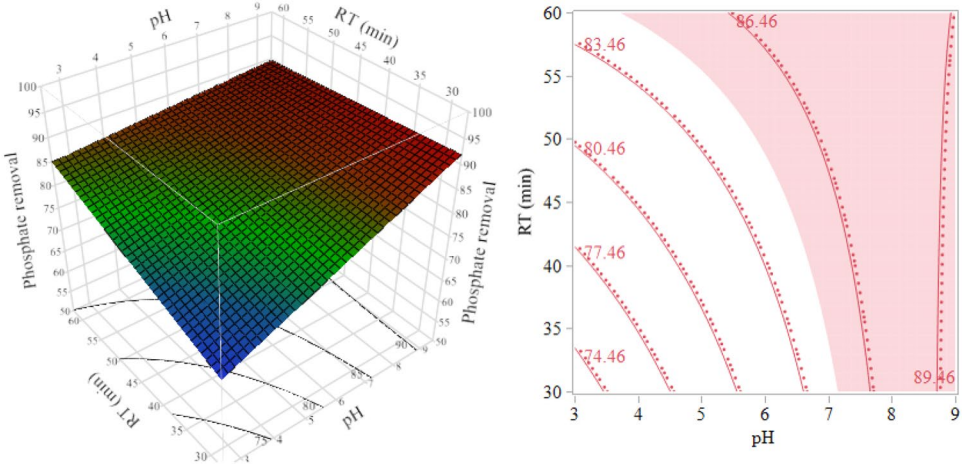

Fig. 7 Two-dimension contour and response surface plots for interaction between pH and RT with other value fixed to center points

reduction of phosphate up to 90%. This can be explained by the presence of more stable iron hydroxides at higher pH which enables the removal of phosphate by adsorption as discussed on the above subsection of `Influence of the pH`.

In the suggested model of phosphate removal (Table 6), it is observed that current density has not appeared as a single effect within the experimental range conducted (3.5–7 mA cm^{-2}) but rather as an interaction effect with other main effects in reducing phosphate (i.e., with initial phosphate concentration and pH). This three-term interaction as 1 effect term has a positive value of the estimate (Table 6), that means increasing the value, increasing the removal of phosphate from the wastewater.

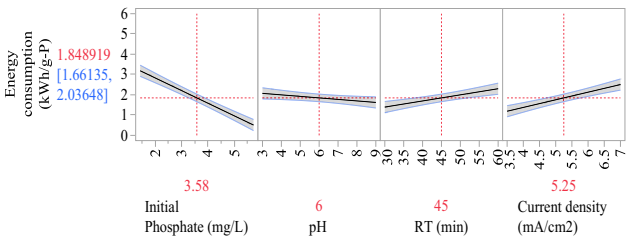

Fig. 8 Prediction profiler of energy consumption for phosphate removal (The vertical red lines correspond to the current value of the factors. The current value of each factor is also shown in red below the horizontal axis. The red value on the vertical axis is the predicted response based on the current values of the factors)

Energy Consumption in the Phosphate Removal Process

The feasibility study of the electrochemical process in large scale application largely depends on electric energy consumption per load of removed pollutants (Karamati-Niaragh et al. 2019). Results of this study showed that the efficiency of phosphate removal in the peroxi-photoelectrocoagulation process reached 97.91% and the electric energy consumed ranges 0.27–5.94 kWh/g-P. The electric energy consumption per a load of removed phosphate was found to depend

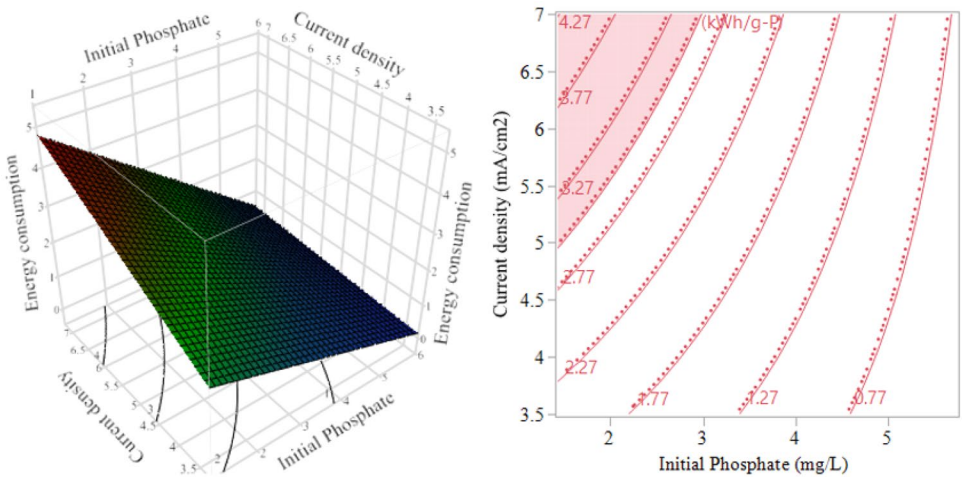

Fig. 9 Two-dimension contour and response surface plots for interaction between initial phosphate and current density with other value fixed to center points

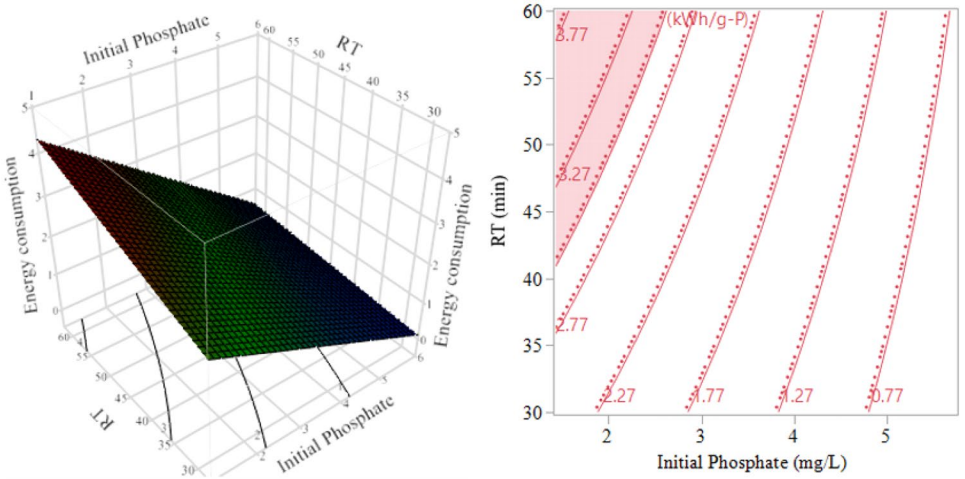

Fig. 10 Two-dimension contour and response surface plots for interaction between initial phosphate and RT with other value fixed to center points

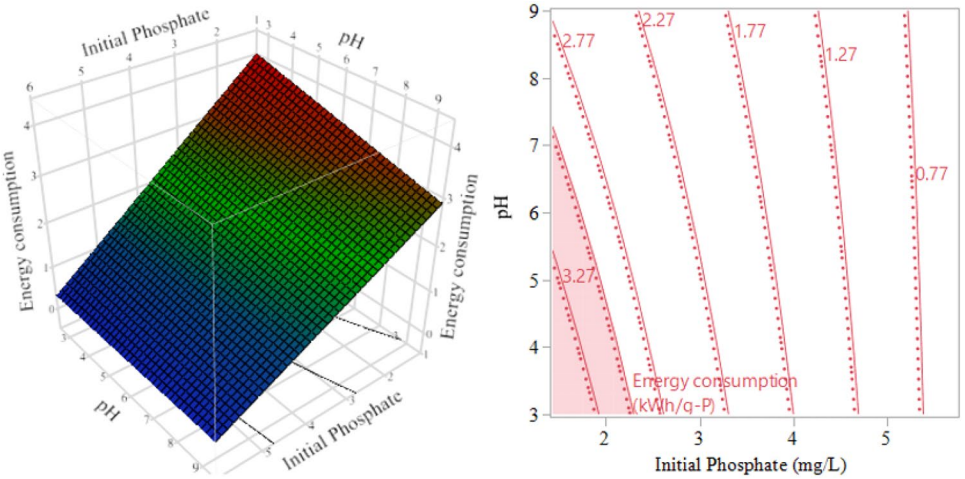

Fig. 11 Two-dimension contour and response surface plots for interaction between initial phosphate and pH with other value fixed to center points

on the initial phosphate concentration, pH, RT and current density (Fig. 8).

The two-dimension contour and response surface plots present visual results of the interactive variables influence on energy consumption (Figs. 9, 10, 11). Figures 8 and 9 shows that energy consumption increased linearly with rising current density and reaction time. The interaction of initial phosphate concentration and pH was also observed

to have a significant effect on the energy expenditure (Fig. 11). In the process of phosphate removal, lower energy expenditure was obtained for a shorter reaction time, a smaller current density and a higher initial phosphate concentration. A similar observation was obtained in research work of Rodziewicz et al. (2020).

Conclusion

The treatment of healthcare wastewater containing phosphate by peroxi-photoelectrocoagulation using electrodes of stainless steel has been studied in a batch reactor. Phosphate removal efficiency has been investigated for a combination of different values of the operating parameters: initial phosphate concentration, the amount of H_2O_2 added, reaction time, current density and initial pH of the wastewater. The result obtained from 37 experiment runs shows that the percentage removal of phosphate range 38.46–97.91% and the concentration of phosphate dropped up to the level of 0.12 mg L^{-1}. The removal efficiency is directly proportional to the initial concentration of phosphate, where the removal efficiency increases with the initial concentration of phosphate. In this process for phosphate removal was increased with pH. It is observed that current density has not appeared as a single effect within the experimental range conducted (3.5–7 mA cm^{-2}) but rather as an interaction effect with other main effects in reducing phosphate (i.e., with initial phosphate concentration and pH). The electric energy consumed in the treatment processes ranges 0.27–5.94 kWh/g-P. The energy consumption per a load of removed phosphate was found to depend on the initial phosphate concentration, pH, RT and current density.

Acknowledgements Sincere thanks are extended to the NASCERE scholarship program and Jimma University for their financial support for this study.

Declarations

Conflict of interest The authors declare that they have no conflict of interest.

References

Al-Raad AA, Hanafiah MM (2021) Removal of inorganic pollutants using electrocoagulation technology: a review of emerging applications and mechanisms. J Environ Manage 300:113696. https://doi.org/10.1016/j.jenvman.2021.113696

APHA (2017) Standard Methods for the examination of Water and wastewater

Attour A, Ben Grich N, Mouldi Tlili M et al (2016) Intensification of phosphate removal using electrocoagulation treatment by continuous pH adjustment and optimal electrode connection mode. Desalin Water Treat 57:13255–13262. https://doi.org/10.1080/19443994.2015.1057537

Besharati Fard M, Mirbagheri SA, Pendashteh A (2020) Removal of TCOD and phosphate from slaughterhouse wastewater using Fenton as a post-treatment of an UASB reactor. J Environ Heal Sci Eng 18:413–422. https://doi.org/10.1007/s40201-020-00469-w

Bouamra F, Drouiche N, Abdi N et al (2018) Removal of phosphate from wastewater by adsorption on marble waste: effect of process parameters and kinetic modeling. Int J Environ Res 12:13–27. https://doi.org/10.1007/s41742-018-0065-3

Bucchianico Di A (2014) Coefficient of determination (R 2). Wiley StatsRef Stat Ref Online. https://doi.org/10.1002/9781118445112.stat03980

Chen Y, Liu C, Guo L et al (2018) Removal and recovery of phosphate anion as struvite from wastewater. Clean Technol Environ Policy 20:2375–2380. https://doi.org/10.1007/s10098-018-1607-2

Cui J, Jin Z, Wang Y et al (2021) Mechanism of eutrophication process during algal decomposition at the water/sediment interface. J Clean Prod 309:127175. https://doi.org/10.1016/j.jclepro.2021.127175

Đuričić T, Bijelić D, Malinović B (2016) The phosphate removal efficiency electrocoagulation wastewater using iron and aluminum electrodes. Bull Chem Technol Bosnia Herzegovina 47:33–38

Fekadu S, Alemayehu E, Dewil R, Van der Bruggen B (2021a) Electrochemical degradation of antivirus drug lamivudine formulation: photoelectrocoagulation, peroxi-electrocoagulation, and peroxi-photoelectrocoagulation processes. J Appl Electrochem 51:607–618. https://doi.org/10.1007/s10800-020-01521-1

Fekadu S, Alemayehu E, Oljira B et al (2021b) Treatment of healthcare wastewater using the peroxi-photoelectrocoagulation process: predictive models for COD, color removal and electrical energy consumption. J Water Process Eng 41:102068. https://doi.org/10.1016/j.jwpe.2021.102068

Hashim KS, Al Khaddar R, Jasim N et al (2019) Electrocoagulation as a green technology for phosphate removal from river water. Sep Purif Technol 210:135–144. https://doi.org/10.1016/j.seppur.2018.07.056

Jung K-W, Hwang M-J, Ahn K-H, Ok Y-S (2015) Kinetic study on phosphate removal from aqueous solution by biochar derived from peanut shell as renewable adsorptive media. Int J Environ Sci Technol 12:3363–3372. https://doi.org/10.1007/s13762-015-0766-5

Karamati-Niaragh E, Alavi Moghaddam MR, Emamjomeh MM, Nazlabadi E (2019) Evaluation of direct and alternating current on nitrate removal using a continuous electrocoagulation process: economical and environmental approaches through RSM. J Environ Manage 230:245–254. https://doi.org/10.1016/j.jenvman.2018.09.091

Lacasa E, Cañizares P, Sáez C et al (2011) Electrochemical phosphates removal using iron and aluminium electrodes. Chem Eng J 172:137–143. https://doi.org/10.1016/j.cej.2011.05.080

Lee J, Rai PK, Jeon YJ et al (2017) The role of algae and cyanobacteria in the production and release of odorants in water. Environ Pollut 227:252–262. https://doi.org/10.1016/j.envpol.2017.04.058

Lin S-S, Shen S-L, Zhou A, Lyu H-M (2021) Assessment and management of lake eutrophication: a case study in Lake Erhai. China Sci Total Environ 751:141618. https://doi.org/10.1016/j.scitotenv.2020.141618

Mahdavi S, Akhzari D (2016) The removal of phosphate from aqueous solutions using two nano-structures: copper oxide and carbon tubes. Clean Technol Environ Policy 18:817–827. https://doi.org/10.1007/s10098-015-1058-y

Mahmud MAP, Ejeian F, Azadi S et al (2020) Recent progress in sensing nitrate, nitrite, phosphate, and ammonium in aquatic

environment. Chemosphere 259:127492. https://doi.org/10.1016/j.chemosphere.2020.127492
Mazloomi S, Yousefi M, Nourmoradi H, Shams M (2019) Evaluation of phosphate removal from aqueous solution using metal organic framework; isotherm, kinetic and thermodynamic study. J Environ Heal Sci Eng 17:209–218. https://doi.org/10.1007/s40201-019-00341-6
Mohan D, Sarswat A, Ok YS, Pittman CU (2014) Organic and inorganic contaminants removal from water with biochar, a renewable, low cost and sustainable adsorbent – a critical review. Bioresour Technol 160:191–202. https://doi.org/10.1016/j.biortech.2014.01.120
Ouslimane T, Aoudj S, Amara M, Drouiche N (2017) Removal of copper and fluoride from mixed Cu-CMP and fluoride-bearing wastewaters by electrocoagulation. Int J Environ Res 11:677–684. https://doi.org/10.1007/s41742-017-0058-7
Pulkka S, Martikainen M, Bhatnagar A, Sillanpää M (2014) Electrochemical methods for the removal of anionic contaminants from water: a review. Sep Purif Technol 132:252–271. https://doi.org/10.1016/j.seppur.2014.05.021
Rodziewicz J, Mielcarek A, Janczukowicz W, Bryszewski K (2020) Electric power consumption and current efficiency of electrochemical and electrobiological rotating disk contactors removing nutrients fromwastewater generated in soil-less plant cultivation systems. Water (switzerland) 12:213. https://doi.org/10.3390/w12010213
SEMATECH N (2003) Engineering statistics handbook
Šikić T, Welles L, Rubio-Rincón FJ et al (2019) Assessment of enhanced biological phosphorus removal implementation potential in a full-scale wastewater treatment plant in croatia. Int J Environ Res 13:1005–1013. https://doi.org/10.1007/s41742-019-00234-4
Tian Y, He W, Zhu X et al (2017) Improved electrocoagulation reactor for rapid removal of phosphate from wastewater. ACS Sustain Chem Eng 5:67–71. https://doi.org/10.1021/acssuschemeng.6b01613
USEPA (1986) Quality Criteria for Water 1986
Verlicchi P, Galletti A, Petrovic M, BarcelÓ D (2010) Hospital effluents as a source of emerging pollutants: an overview of micropollutants and sustainable treatment options. J Hydrol 389:416–428. https://doi.org/10.1016/j.jhydrol.2010.06.005
Verlicchi P, Aukidy M Al, Chalabi S Al (2018) The Handbook of Environmental Chemistry Characteristics, Management, Treatment and Environmental Risks
Yang Y, Zhang L, Shao H et al (2017) Enhanced nutrients removal from municipal wastewater through biological phosphorus removal followed by partial nitritation/anammox. Front Environ Sci Eng. https://doi.org/10.1007/s11783-017-0911-0
Zhang J, Bligh MW, Liang P et al (2018) Phosphorus removal by in situ generated Fe(II): efficacy, kinetics and mechanism. Water Res 136:120–130. https://doi.org/10.1016/j.watres.2018.02.049
Zuthi MFR, Guo WS, Ngo HH et al (2013) Enhanced biological phosphorus removal and its modeling for the activated sludge and membrane bioreactor processes. Bioresour Technol 139:363–374. https://doi.org/10.1016/j.biortech.2013.04.038

Authors and Affiliations

Samuel Fekadu[1,2,4] · Esayas Alemayehu[2,5] · Perumal Asaithambi[2] · Bart Van der Bruggen[1,3]

[1] Department of Chemical Engineering, Process Engineering for Sustainable Systems Section, KU Leuven, Celestijnenlaan 200f-box 2424, 3001 Leuven, Belgium

[2] Faculty of Civil and Environmental Technology, Jimma Institute of Technology, Jimma University, Po Box-378, Jimma, Ethiopia

[3] Faculty of Engineering and the Built Environment, Tshwane University of Technology, Private Bag X680, Pretoria 0001, South Africa

[4] Department of Environmental Health Science and Technology, Jimma University, Po Box-378, Jimma, Ethiopia

[5] Africa Center of Excellence for Water Management, Addis Ababa University, Po Box-1176, Addis Ababa, Ethiopia